where an exothermic reaction occurred. After 1 h at 25 °C, all volatile materials were evacuated to leave a white solid, CF_3CH_2OLi (20 mmol, 2.1 g, ~100%).

Preparation of 2,2,2-Trifluoroethyl Dichlorophosphinite, $CF_3CH_2OPCl_2$. Onto CF_3CH_2OLi (20 mmol, 2.1 g) in a 1000-mL round-bottomed Pyrex flask at −196 °C, was condensed PCl_3 (20 mmol, 2.75 g). This flask was warmed to and held at 25 °C for 10 h. Trap-to-trap distillation gave $CF_3CH_2OPCl_2$ (13 mmol, 2.6 g, 65% yield) in a trap at −45 °C, PCl_3 in a trap at −120 °C, and a mixture of $(CF_3CH_2O)_2PCl$ and $(CF_3CH_2O)_3P$ in a trap at −30 °C.

Preparation of Bis(polyfluoroalkyl) Chlorophosphonites, $(R_fO)_2PCl$, or Tris(polyfluoroalkyl) Phosphites, $(R_fO)_3P$. This preparation can be carried out as described above for polyfluoroalkyl dichlorophosphinites, except the stoichiometry of the reaction is 2:1 of R_fOLi to PCl_3 or 3:1 of R_fOLi to PCl_3.

Preparation of $(R_fO)P(O)Cl_2$, $(R_fO)_2P(O)Cl$, and $(R_fO)_3PO$. The compound, R_fOPCl_2 or $(R_fO)_2PCl$ (5 mmol), was transferred into a 100-mL flask equipped with a Teflon stopcock. Stoichiometric amounts of N_2O_4 were condensed at −196 °C onto the compound. The oxidation was complete at low temperatures from −50 to −20 °C. The trap-to-trap distillation gave the products in their respective traps. For $(R_fO)_3P$, the starting material was transferred to the 100-mL flask under an inert atmosphere. After the flask was evacuated at −196 °C, the stoichiometric amount of N_2O_4 was transferred and the temperature was raised from −196 to +25 °C slowly. After 1 h the volatile materials, including NO, were removed, leaving behind a very slightly volatile liquid or solid.

Preparation of $(R_fO)_2P(O)Cl$ from $(R_fO)_3P + Cl_2$. The tris(polyfluoroalkyl) phosphites (5 mmol) were transferred into a 100-mL round-bottomed flask under an inert atmosphere. After the flask was evacuated at −196 °C, Cl_2 (5 mmol) was condensed in. The temperature was raised to 25 °C slowly and left there for a few hours. The trap-to-trap distillation gave the $(R_fO)_2P(O)Cl$ compounds in their respective traps as described earlier.

Hydrolysis of Polyfluoroalkyl Dichlorophosphinates ($R_fOP(O)Cl_2$), Bis(polyfluoroalkyl) Chlorophosphonates ($(R_fO)_2P(O)Cl$), and $(R_fO)_3PO$. The hydrolysis of these phosphates to form acid phosphates, $(R_fO)_2P(O)OH$, was carried out by condensing distilled water onto the dichlorophosphinates, chlorophosphonates, or tris(polyfluoroalkyl) phosphates. The reaction proceeded smoothly for the dichlorophosphinates at room temperature, whereas the reaction between $(R_fO)_2P(O)Cl$ and H_2O took place in the range of 50–64 °C. The reaction was also smooth between $[(CF_3)_2CHO]_3PO$ and water at ambient temperature, and for $[CF_3(CH_3)CHO]_3PO$ and H_2O at 68 °C. Freeze-drying gave the acid phosphates $R_fOP(O)(OH)_2$ and $(R_fO)_2P(O)OH$.

Preparation of $CF_3CH_2OP(O)(\mu\text{-}O)_2P(O)OCH_2CF_3$. $CF_3CH_2OPCl_2$ (1.0 g, 5 mmol) was transferred into a 1000-mL round-bottomed flask equipped with a Teflon stopcock at −196 °C. Then N_2O_4 (1.12 g, 12 mmol) was condensed onto the $CF_3CH_2OPCl_2$. The reaction mixture was warmed to and left at 25 °C overnight. The trap-to-trap distillation gave NOCl in a trap at −196 °C, N_2O_3 at −140 °C, and

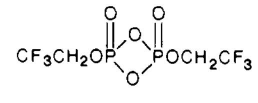

in a trap at −25 °C in ~100% yield. This compound was characterized by its ^1H, ^{19}F and ^{31}P NMR spectra as well as by its mass spectrum.

Acknowledgment is expressed to the donors of the Petroleum Research Fund administered by the American Chemical Society, to the National Science Foundation (Grant CHE-8404974), to the Air Force Office of Scientific Research (Grant 82-0247), and to the Gas Research Institute for support of this research. We thank Dr. Gary Knerr for mass spectral data.

Registry No. $(CF_3CH_2O)_2P(O)OH$, 40547-38-4; $[H(CF_2)_4CH_2O]_2P(O)OH$, 2794-65-2; $[(CF_3)_2CHO]_2P(O)OH$, 103981-52-8; $[CF_3(CH_3)CHO]_2P(O)OH$, 103981-53-9; $[CF_3(CH_3)_2CO]_2P(O)OH$, 103981-54-0; $[(CF_3)_2CH_3CO]_2P(O)OH$, 103981-55-1; $CF_3CH_2OP(O)(OH)_2$, 2805-15-4; $(CF_3)_2CHOP(O)(OH)_2$, 101686-67-3; $CF_3(CH_3)CHOP(O)(OH)_2$, 103981-56-2; $CF_3(CH_3)_2COP(O)(OH)_2$, 103981-57-3; $[CF_3(CH_3)_2COP(O)(OH)]_2O$, 103981-58-4; $(CF_3)_2CH_3COP(O)(OH)_2$, 104013-77-6; $[(CF_3)_2CH_3COP(O)(OH)]_2O$, 103981-59-5; $CF_3CH_2OP(O)(\mu\text{-}O)_2P(O)OCH_2CF_3$, 103981-60-8; $(CF_3CH_2O)_2P(O)Cl$, 381-44-2; CF_3CH_2OH, 75-89-8; $(CF_3CH_2O)_3PO$, 358-63-4; $[H(CF_2)_4CH_2O]_3PO$, 355-86-2; $[(CF_3)_2CHO]_3PO$, 66489-68-7; $[CF_3(CH_3)CHO]_3PO$, 103981-61-9; $[CF_3(CH_3)CHO]_2P(O)Cl$, 103981-62-0; $[CF_3(CH_3)_2CO]_2P(O)Cl$, 103981-63-1; $[(CF_3)_2CH_3CO]_2P(O)Cl$, 103981-64-2; $CF_3CH_2OP(O)Cl_2$, 462-56-6; $(CF_3)_2CHOP(O)Cl_2$, 103981-65-3; $CF_3(CH_3)CHOP(O)Cl_2$, 103981-66-4; $CF_3(CH_3)_2COP(O)Cl_2$, 103981-67-5; $(CF_3)_2CH_3COP(O)Cl_2$, 103981-68-6; $CF_3CH_2OPCl_2$, 103981-69-7; $(CF_3)_2CHOPCl_2$, 67091-84-3; $[(CF_3)_2CHO]_2PCl$, 67091-85-4; $[(CF_3)_2CHO]_3P$, 66470-81-3; $(CF_3)_2CH_3COPCl_2$, 103981-70-0; $CF_3(CH_3)_2COPCl_2$, 103981-71-1; $CF_3(CH_3)CHOPCl_2$, 103981-72-2; $[(CF_3)_2CH_3CO]_2PCl$, 103981-73-3; $[CF_3(CH_3)_2CO]_2PCl$, 103981-74-4; $[(CF_3)_2CH_3CO]_3P(O)$, 103981-75-5; $[CF_3(CH_3)_2CO]_3P$, 103981-76-6; $[CF_3(CH_3)CHO]_3P$, 79155-02-5; $[(CF_3(CH_3)_2CO)_2P(O)]_2O$, 103981-77-7; $(CF_3(CH_3)_2CO)_2P(O)H$, 103981-78-8; $[(CF_3)_2CHO]_3PCl_2$, 66559-58-8; CF_3CH_2OLi, 69163-14-0; $(CF_3)_2CHOLi$, 29649-10-3; $(CF_3)_2CHOH$, 920-66-1; $(CF_3)_2CH_3COLi$, 98171-13-2; $(CF_3)(CH_3)_2COLi$, 102828-97-7; $CF_3(CH_3)CHOLi$, 103981-79-9; $CF_3(CH_3)_2COLi$, 102828-97-7; $CF_3(CH_3)CHOH$, 374-01-6; $(CF_3CH_2O)_3P$, 370-69-4; $[CF_3(CH_3)_2CO]_2P(O)H$, 103981-78-8; $CF_3(CH_3)_2COH$, 507-52-8; $[(CF_3)_2CH_3CO]_3P$, 103981-80-2; CF_3CH_2Cl, 75-88-7; $CF_3(CH_3)C{=}CH_2$, 374-00-5; $[[(CF_3)_2CH_3CO]_2P(O)]_2O$, 103981-81-3; $(CF_3)_2C{=}CH_2$, 382-10-5; $CF_3(CH_3)CHCl$, 460-35-5.

Notes

Contribution from the Department of Chemistry,
West Virginia University, Morgantown, West Virginia 26506

Direct Evidence for an S_N1CB Mechanism. 4. Crystal and Molecular Structure of Chloro(bis(8-quinolinyl)amido-N^1,N^2,N^3)copper(II), a Metal Chelate Containing an sp^2-Hybridized Deprotonated Amine

Jeffrey P. Puzas, Robert Nakon,* and Jeffrey L. Petersen*

Received April 7, 1986

As possible models for substrate release at metalloenzyme centers, we have reported aminoacidate dechelation upon amide deprotonation[1] in the bis(N-acetamidoiminodiacetato)copper(II) chelate $[Cu(ADA)_2{}^{2-}]$ (eq 1), upon hydroxy group ionization[2] in the bis(N,N-bis(2-hydroxyethyl)glycinato)copper(II) chelate (eq 2), and upon peptide proton ionization[3] in the mixed-ligand chelate

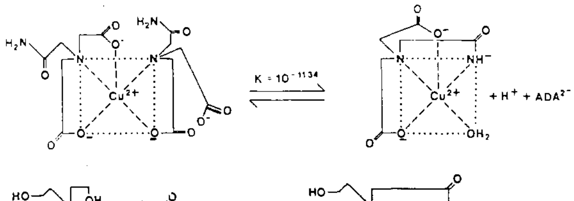

(1)

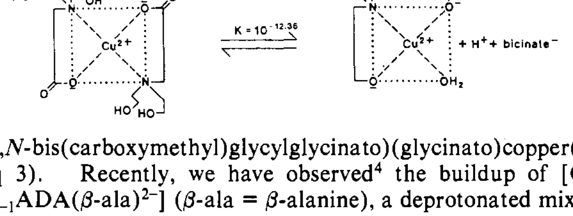

(2)

(N,N-bis(carboxymethyl)glycylglycinato)(glycinato)copper(II) (eq 3). Recently, we have observed[4] the buildup of $[Cu(H_{-1}ADA(\beta\text{-ala})^{2-}]$ (β-ala = β-alanine), a deprotonated mixed-ligand chelate, in solution prior to the release of β-alanine. This work was predicated on the belief that the S_N1CB mechanism,

---

[1] Paar, D. P.; Rhodes, C. R., III; Nakon, R. *Inorg. Chim. Acta* **1983**, *80*, L11.

[2] Krishnamoorthy, C. R.; Nakon, R. *Inorg. Chim. Acta* **1983**, *80*, L33.

[3] Nakon, R.; Krishnamoorthy, C. R. *J. Am. Chem. Soc.* **1984**, *106*, 5193.

[4] Nakon, R.; Krishnamoorthy, C. R.; Townshend, S.; Grayson, J. *Inorg. Chim. Acta* **1986**, *124*, L5.

0020-1669/86/1325-3837$01.50/0

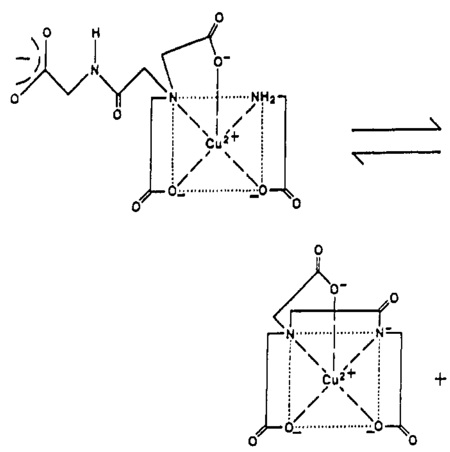

(3)

as developed by Basolo and Pearson[5] for Co(III) substitution reactions in basic solutions (eq 4), could also be operative in those of Cu(II) as well as other metal ions.

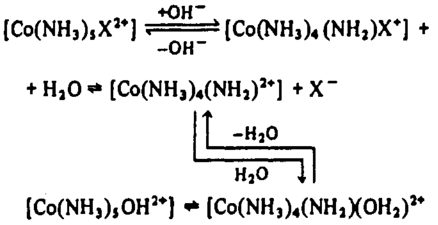

$$[Co(NH_3)_5X^{2+}] \underset{-OH^-}{\overset{+OH^-}{\rightleftharpoons}} [Co(NH_3)_4(NH_2)X^+] + \; + H_2O \rightarrow [Co(NH_3)_4(NH_2)^{2+}] + X^- \quad \xrightarrow{-H_2O} \quad \xleftarrow{H_2O} \quad [Co(NH_3)_5OH^{2+}] \leftarrow [Co(NH_3)_4(NH_2)(OH_2)^{2+}]$$

(4)

Basolo and Pearson[6] originally proposed that the strong labilizing effects of the NH_2^- residue were due either to the ability of this group to π-bond to the metal as in I (which would arise

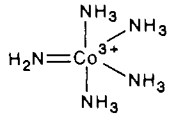

I

from $[Co(NH_3)_5X^{2+}]$) or to its strong basicity. In an elegant experiment, Sargeson and co-workers[7] showed that the asymmetric N trans to the chloride leaving group in II underwent racemization

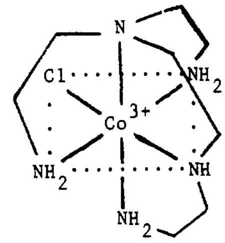

II

at a much slower rate than did base hydrolysis. Therefore, base hydrolysis did not occur through a symmetrical π-bond sp^2 N as shown in I, and the lability of deprotonated amine species appears to be due to the very strong basicity of the NH_2^- ligand. Therefore, we decided to synthesize a Cu(II) chelate containing an ionized amine group in which the nitrogen would by necessity be planar and therefore sp^2 hybridized, which is required by the sterochemistry of ionized amide or peptide groups. If the Cu–Cl bond trans to the ionized amine group was longer than normal, a ground-state kinetic effect would be indicated.

Experimental Section

Syntheses. The ligand, bis(8-quinolinyl)amine (DQA), was synthesized by a modified Bucherer reaction.[8] A suspension of 8-aminoquinoline (28 g), sodium pyrosulfite (120 g), and an excess of 8-hydroxyquinoline (45 g) in 500 mL of H_2O was refluxed and mechanically stirred for 1 week. The mixture was then cooled and treated with 1.0 L of 2 M NaOH, and the remaining solid was collected on a filter and washed with H_2O until neutral. Excess 8-aminoquinoline was removed by steam distillation, and the remaining solid was purified by recrystallization from toluene/ethanol and then from hexane. The yield was 4.2 g (8%) of long, yellow needles (mp 134–135 °C, uncorrected; lit.[8] mp 132.7–133.4 °C).

Table I. Data for X-ray Diffraction Analysis of $Cu(C_{18}N_3H_{12})Cl$

A. Crystal Data	
cryst syst	monoclinic
space group	$P2_1/n$
a, Å	12.683 (3)
b, Å	15.050 (4)
c, Å	7.542 (2)
β, deg	91.15 (2)
V, Å³	1439.4 (7)
fw	369.31
d(calcd), g/cm³	1.704
Z	4
μ, cm⁻¹	17.61
B. Data Collection and Analysis Summary	
cryst dimens, mm	0.288 × 0.175 × 0.625
reflcns sampled	±hkl (5 ≤ 2θ ≤ 50°)
2θ range for centered reflcns, deg	30 < 2θ < 35
scan rate, deg min⁻¹	2.0
scan width, deg	1.1 + 0.9(tan θ)
no. of std reflcns	3
% cryst decay	0
total no. of measd reflcns	2743
no. of unique data used	2538 ($F_o^2 > 0$)
agreement between equiv data	
$R_{av}(F_o)$	0.016
$R_{av}(F_o^2)$	0.015
transmissn coeff	0.619–0.741
P	0.025
discrepancy indices	
$R(F_o)$	0.038
$R(F_o^2)$	0.042
$R_w(F_o^2)$	0.066
σ_1	1.54
no. of variables	257
data to param ratio	9.88:1

The copper complex, $[Cu(H_{-1}DQA)Cl]$ was synthesized by adding 0.24 g of DQA dissolved in THF to 0.075 g of $CuCl_2 \cdot 2H_2O$ (Fisher Scientific) dissolved in H_2O. With stirring, 0.05 g of KOH (Fisher Scientific) was then added, and a red precipitate immediately formed. THF was added until the precipitate dissolved. The solution was set aside in the dark. Within 1 week, large platelets formed. The platelets were dissolved in a minimum amount of chloroform and the beaker placed in a larger one containing toluene and sealed. After several weeks in the dark, large (2–6 cm) dark needles formed.

X-ray Diffraction Measurements for $Cu(C_{18}N_3H_{12})Cl$. A dark-red rectangular crystal (obtained by cleaving a long needle) was wedged along the growth axis into a glass capillary tube, sealed, and then transferred to a Picker goniostat that is controlled by a Krisel Control diffractometry automation system. Procedures similar to those described previously[9] were employed to determine the lattice parameters and collect the X-ray diffraction data. Specific details are summarized in Table I. The systematic absences of {h0l}, $h + l = 2n + 1$, and {0k0}, $k = 2n + 1$, are consistent with $P2_1/n$, a nonstandard setting of $P2_1/c$ (No. 14, C_{2h}^5).

Intensity data were measured with Zr-filtered Mo Kα X-ray radiation with a takeoff angle of 2°. The θ–2θ scan mode was employed with a fixed scan rate and a variable scan width, ω. Background counts of 10-s duration were measured at the extremes of each scan with the crystal and detector being stationary. The combined intensity of three standard reflections that were measured after every 90 min of exposure provided no indication of crystal deterioration. To correct for possible detector saturation, the more intense reflections were remeasured with a precalibrated attentuator inserted in front of the detector apeture.

The integrated intensity, I, and its standard deviation, $\sigma_c(I)$, for each of the measured peaks were calculated from the expressions $I = \omega(S/t_s$

---

[5] Basolo, F.; Pearson, R. G. *Nature (London)* **1962**, *194*, 177.

[6] Pearson, R. G.; Basolo, F. *J. Am. Chem. Soc.* **1956**, *78*, 4878.

[7] Buckingham, D. A.; Marzilli, P. A.; Sargeson, A. M. *Inorg. Chem.* **1969**, *8*, 1595.

[8] Jensen, K. A.; Nielson, P. H. *Acta Chem. Scand.* **1964**, *18*, 1.

[9] Nicholson, G. A.; Petersen, J. L.; McCormick, B. J. *Inorg. Chem.* **1982**, *21*, 3274.

Table II. Positional Parameters for $Cu(C_{18}N_3H_{12})Cl^a$

atom	x	y	z
Cu	0.50425 (2)	0.39588 (2)	0.63926 (4)
Cl	0.45576 (5)	0.25726 (4)	0.56943 (11)
N1	0.6551 (1)	0.3819 (1)	0.5812 (2)
N2	0.5512 (1)	0.5121 (1)	0.7173 (3)
N3	0.3667 (1)	0.4381 (1)	0.7279 (3)
C1	0.7022 (2)	0.3139 (2)	0.5042 (3)
C2	0.8103 (2)	0.3107 (2)	0.4820 (4)
C3	0.8709 (2)	0.3782 (2)	0.5427 (4)
C4	0.8247 (2)	0.4529 (2)	0.6210 (3)
C5	0.7140 (2)	0.4530 (1)	0.6361 (3)
C6	0.8817 (2)	0.5291 (2)	0.6786 (4)
C7	0.8279 (2)	0.5998 (2)	0.7415 (4)
C8	0.7178 (2)	0.6007 (2)	0.7545 (3)
C9	0.6578 (2)	0.5269 (2)	0.7087 (3)
C10	0.4760 (2)	0.5619 (2)	0.8022 (3)
C11	0.4837 (2)	0.6438 (2)	0.8819 (4)
C12	0.3964 (2)	0.6842 (2)	0.9605 (4)
C13	0.2999 (2)	0.6456 (2)	0.9603 (4)
C14	0.2861 (2)	0.5619(2)	0.8803 (3)
C15	0.3744 (2)	0.5200 (2)	0.8049 (3)
C16	0.1897 (2)	0.5163 (2)	0.8701 (4)
C17	0.1835 (2)	0.4355 (2)	0.7916 (4)
C18	0.2734 (2)	0.3975 (2)	0.7223 (4)
H1	0.661 (2)	0.274 (2)	0.460 (3)
H2	0.839 (2)	0.267 (2)	0.421 (3)
H3	0.946 (2)	0.379 (2)	0.531 (3)
H4	0.957 (2)	0.525 (2)	0.682 (3)
H5	0.864 (2)	0.648 (2)	0.771 (3)
H6	0.686 (2)	0.652 (2)	0.786 (3)
H7	0.544 (2)	0.672 (2)	0.881 (4)
H8	0.407 (2)	0.737 (2)	1.019 (3)
H9	0.244 (2)	0.671 (2)	1.014 (3)
H10	0.133 (2)	0.540 (2)	0.914 (4)
H11	0.120 (2)	0.404 (2)	0.780 (4)
H12	0.273 (2)	0.345 (2)	0.669 (3)

[a] The estimated standard deviation in parentheses for this and all subsequent tables refer to the least significant figures.

$- B/t_b)$ and $\sigma_c(I) = \omega(S/t_s^2 + B/t_b^2)^{1/2}$, where S represents the scan count accumulated in time t_s and B is the combined background count in time t_b. The data was corrected for absorption and Lorentz–polarization effects. The standard deviation of the square of each structure factor, $F_o^2 = I/Lp$, was calculated from $\sigma(F_o^2) = [\sigma_c^2(F_o^2) + (pF_o^2)^2]^{1/2}$. Duplicate reflections were averaged to provide 2538 unique reflections, which were all used in the structural analysis.

Structural Analysis. An initial position for the Cu atom was obtained from an interpretation of an unsharpened three-dimensional Patterson map. A subsequent Fourier summation provided approximate coordinates for all the remaining non-hydrogen atoms. Following a refinement of the positional parameters and corresponding anisotropic temperature factors, a difference Fourier synthesis utilizing only low-angle data ($\sin \theta)/\lambda < 0.40$ Å^{-1}) was used to determine approximate coordinates for all of the hydrogen atoms. Prior to the final refinement an examination of the agreement between F_o and F_c indicated a consistent systematic variation due to extinction for the more intense reflections, such as 122. An isotropic secondary extinction parameter, g, was introduced into the refinement to correct for this effect. Full-matrix least-squares refinement (based on F_o^2) with anisotropic temperature factors for the 23 non-hydrogen atoms and isotropic temperature factors for the 12 hydrogen atoms converged to the final discrepancy indices given in Table I with $g = (2.7\ (4)) \times 10^{-5}$. A final difference Fourier map did not contain any residuals greater than 0.2 e/Å^3 and thereby verified the completeness of the structural refinement.

The values for the positional parameters and temperature factors obtained from the last least-squares cycle for all of the atoms are provided in Table II. Interatomic distances and bond angles for the non-hydrogen atoms with their corresponding esd's are presented in Table III. Tables of the temperature factors, the hydrogen atom distances and angles, and pertinent least-square planes and a table of observed and calculated structure factors are available as supplementary material. The computer programs that were used for the structural analysis have been described previously.[10]

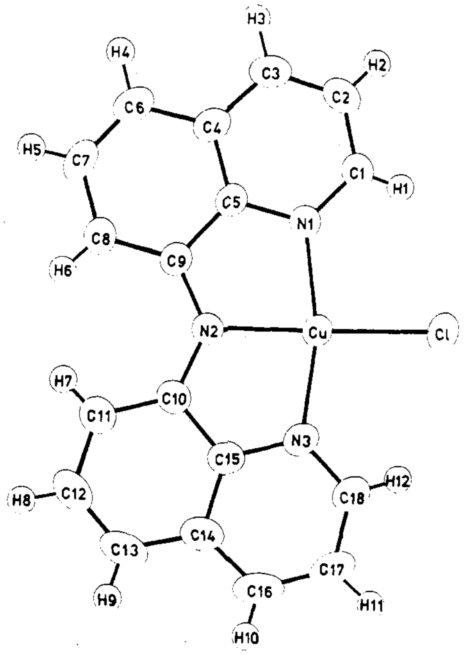

Figure 1. Perpsective view of the molecular structure of $Cu(C_{18}N_3H_{12})Cl$ with the atom-labeling scheme. The thermal ellipsoids are scaled to enclose 50% probability. For clarity the radii of the spheres for the hydrogen atoms were arbitrarily reduced.

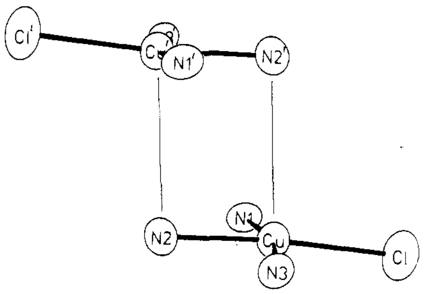

Figure 2. Coordination environment about copper atom in $Cu(C_{18}N_3H_{12})Cl$ depicting occupation of an apical coordination site by N2 of a symmetry-related (primed) molecule. Pertinent distances and angles include the following: Cu···N2′, 3.093 (2) Å, Cl–Cu···N2′, 99.0 (1)°; N1–Cu···N2′, 93.4 (1)°; N2–Cu···N2′, 94.4 (1)°; N3–Cu···N2′, 87.9 (1)°.

Results and Discussion

Description of the Molecular Structure of $Cu(H_{-1}DQA)Cl$. The molecular structure of $Cu(C_{18}N_3H_{12})Cl$ (or $Cu(H_{-1}DQA)Cl$) with the corresponding atom-labeling scheme is depicted in Figure 1. A closer examination of the molecular packing, however, reveals the presence of a pairwise interaction between monomer units in the solid state. As shown in Figure 2, each ionized amine group (N2,N2′) clearly occupies an apical coordination site of the second Cu(II) center (Cu′, Cu) and thereby produces a square-pyramidal geometry about each metal. The sp^2 hybridization about each ionized amine group, as reflected by the Cu–N2–C9, Cu–N2–C10, and C9–N2–C10 bond angles of 115.4 (1), 114.9 (2), and 128.6 (2)°, respectively, leaves a filled p_z orbital, which apparently is sufficiently basic to bind to a second copper atom, thereby causing dimerization. However, this interaction produces only a minimal displacement (0.092 Å) of N2 out of the Cu–C9–C10 plane and therefore does not significantly alter the sp^2 hybridization about N2. The repulsion of the π-clouds of the two sets of quinoline moieties, which are situated directly opposite one another in the dimer, is probably a major factor for the rather large N2–Cu′ (N2′–Cu) distance of 3.093 (2) Å. The Cu atom being only slightly displaced by 0.049 Å from the plane determined by the N1, N2, and N3 atoms results in a nearly rectangular array of the four atoms (Cu, Cu′, N2, and N2′) involved in dimer formation. In contrast, the Cl atom is displaced out of this plane

---

(10) Nicholson, G. A.; Petersen, J. L.; McCormick, B. J. *Inorg. Chem.* **1980**, *19*, 195.

Table III. Interatomic Distances (Å) and Bond Angles (deg) for Non-Hydrogen Atoms in $Cu(C_{18}N_3H_{12})Cl$[a]

Interatomic Distances			
Cu–Cl	2.235 (7)	Cu–N2	1.935 (2)
Cu–N1	1.982 (2)	Cu–N3	1.985 (2)
N1–C1	1.325 (3)	N3–C18	1.332 (3)
N1–C5	1.365 (3)	N3–C15	1.366 (3)
N2–C9	1.373 (3)	N2–C10	1.381 (3)
C1–C2	1.387 (4)	C18–C17	1.387 (4)
C2–C3	1.348 (4)	C17–C16	1.353 (5)
C3–C4	1.404 (4)	C16–C14	1.403 (4)
C4–C5	1.411 (3)	C14–C15	1.414 (3)
C4–C6	1.418 (4)	C14–C13	1.407 (4)
C6–C7	1.355 (4)	C13–C12	1.355 (5)
C7–C8	1.402 (4)	C12–C11	1.405 (4)
C8–C9	1.387 (4)	C11–C10	1.373 (4)
C5–C9	1.435 (3)	C15–C10	1.436 (3)
Bond Angles			
Cl–Cu–N1	96.4 (1)	Cl–Cu–N3	98.0 (1)
N1–Cu–N2	82.6 (1)	N3–Cu–N2	82.9 (1)
Cl–Cu–N2	175.4 (1)	N1–Cu–N3	165.2 (1)
Cu–N1–C1	128.6 (2)	Cu–N3–C18	129.0 (2)
Cu–N1–C5	112.0 (1)	Cu–N3–C15	112.1 (1)
C1–N1–C5	119.3 (2)	C18–N3–C15	118.9 (2)
Cu–N2–C9	115.4 (1)	Cu–N2–C10	114.9 (1)
C9–N2–C10	128.6 (2)		
N1–C1–C2	122.4 (2)	N3–C18–C17	122.3 (3)
C1–C2–C3	119.4 (3)	C18–C17–C16	119.7 (3)
C2–C3–C4	120.5 (2)	C17–C16–C14	120.4 (3)
C3–C4–C5	117.3 (2)	C16–C14–C15	117.2 (2)
C3–C4–C6	124.2 (2)	C16–C14–C13	124.2 (3)
C5–C4–C6	118.4 (2)	C15–C14–C13	118.6 (2)
N1–C5–C4	121.0 (2)	N3–C15–C14	121.5 (2)
N1–C5–C9	116.7 (2)	N3–C15–C10	116.6 (2)
C9–C5–C4	122.3 (2)	C10–C15–C14	121.9 (2)
C4–C6–C7	119.0 (2)	C14–C13–C12	119.3 (3)
C6–C7–C8	122.8 (3)	C13–C12–C11	122.2 (3)
C7–C8–C9	121.1 (2)	C12–C11–C10	121.6 (3)
C8–C9–C5	116.2 (2)	C11–C10–C15	116.4 (2)
C8–C9–N2	130.9 (2)	C11–C10–N2	130.3 (2)
C5–C9–N2	113.0 (2)	C15–C10–N2	113.3 (2)

[a] The esd's given in parentheses for the interatomic separations and bond angles were calculated from the standard errors in the fractional coordinates of the corresponding atomic positions.

in the opposite direction by 0.074 Å.

The Cu–ionized amine bond (Cu–N2) distance (1.935 (2) Å) is 0.05 Å shorter than the Cu–quinoline N bond distances. Since the Cu–pyridine N bond distance[9] in (2,6-diacetylpyridine dioxime)copper(II) chloride (1.932 (3) Å) is similar to that of $Cu-N_2$ in $[Cu(H_{-1}DQA)Cl]$, doubt is cast on whether the short bond distance is due to the increased basicity of an ionized amine group. Both ligands, $H_{-1}DQA$ and $DAPDH_2$, are prevented on the basis of steric requirements from bonding to Cu(II) with ideal N–Cu–N bond angles of 90°. In order to position the terminal N donors for optimal bonding, the copper ion is drawn more closely to the central N donor than in the absence of these steric constraints. As a result in $Cu(H_{-1}DQA)Cl$, the C9–N2–C10 bond angle of the tridentate ligand is significantly greater than 120° and is accompanied by internal N–Cu–N bond angles (N1–Cu–N2, 82.6 (1)°; N2–Cu–N3, 82.9 (1)°) that are substantially less than 90°.

Kinetic Implications. The Cu–Cl bond length in $[Cu(H_{-1}DQA)Cl]$ is typical of those found in a wide variety of Cu(II) complexes. Since there is no lengthening of the Cu–Cl bond trans to an ionized amine group it appears that any increase of lability of the chloride ion should not reside in a ground state effect. Since Sargeson's experiment[6] clearly showed that there is no π-stabilization of the transition state and/or intermediate and these data indicate no Cu–Cl bond lengthening, it appears that the high basicity of the ionized amine group would apparently be involved in stabilizing the transition state and/or intermediate of reduced coordination number (eq 4), a necessary feature of the S_N1CB mechanism.

The ability of strong σ-donors to induce stereochemical changes in metal chelates is well documented. Upon ionization of peptide or amide protons in Ni(II) complexes containing polypeptide or polyamide ligands, Ni(II) undergoes a change from an octahedral to a square-planar geometry.[11,12] Similarly, Zn(II) has been proposed to undergo an octahedral to tetrahedral stereochemical change upon amide proton ionization in a Zn(II) chelate.[13] Furthermore, weak σ-donors usually yield octahedral O_h Zn(II) complexes in aqueous solution (H_2O, Cl^-) while strong σ-donors often yield tetrahedral Zn(II) complexes (CN^-).[14] In the latter case, since ligand field effects can be ruled out in a d^{10} system, the increased acidity of a tetrahedral site compared to that of an octahedral one is apparently the driving force for the stereochemical change.[13] Therefore, our current models for substrate release at metalloenzymes centers continue to be in agreement with the features generally attributed to an S_N1CB mechanism.

Acknowledgment. Computer time for the structural refinement and analysis of the X-ray diffraction data was provided by the West Virginia Network for Educational Telecomputing.

Registry No. DQA, 88783-63-5; $[Cu(H_{-1}DQA)Cl]$, 104035-43-0; 8-aminoquinoline, 578-66-5; 8-hydroxyquinoline, 148-24-3.

Supplementary Material Available: Tables of refined thermal parameters, hydrogen bond distances and angles, and pertinent least-squares planes (3 pages); a table of observed and calculated structure factors (9 pages). Ordering information is given on any current masthead page.

---

(11) Martin, R. B.; Chamberlain, M.; Edsall, J. T. *J. Am. Chem. Soc.* **1960**, *82*, 2195.
(12) Bai, K. S.; Martell, A. E. *Inorg. Chem.* **1970**, *9*, 1126.
(13) Lance, E. A.; Nakon, R. *Inorg. Chim. Acta* **1981**, *55*, L1.
(14) Cotton, F. A.; Wilkinson, G. *Advanced Inorganic Chemistry*, 2nd ed.; Wiley: New York, 1966; p 607.

Contribution from the Department of Chemistry,
University of Warwick, Coventry CV4 7AL, U.K.

Physical and Chemical Quenching of Excited Uranyl Ion by Dialkyl Sulfides

Terence J. Kemp* and Mark A. Shand

Received April 2, 1985

A recent paper[1] has dealt with the photochemical reduction of uranyl ion by several dialkyl sulfides. The results described therein intrigued us because (i) we had been working on a closely similar study, which formed the basis of our contribution to a recent Faraday Discussion,[2] (ii) there is a major disagreement concerning the magnitudes of the quantum yields for U(IV) production for the group of compounds in general and for di-*n*-butyl sulfide in particular (see Table I), and (iii) we have ESR evidence for the intermediacy of semioxidized substrate with a sulfur-centered singly occupied molecular orbital in several but not all cases,[2-4] which conflicts with the oxygen atom transfer mechanism proposed in ref 1. Concentrating on point ii, we note there is a possibly significant difference in methodology between the actinometric techniques of Sandhu et al.[5] and ourselves in that whereas the former group use a very broad band of irradiation wavelengths, i.e. the output of a 125-W medium-pressure Hg lamp filtered through Pyrex (the reaction vessel), which is both polychromatic and more intense, we use the output of a current-stabilized 200-W medium-pressure Xe/Hg lamp filtered through a Balzer metal interference filter ($\lambda_{transmitted}$ = 401 ± 20 nm). Both groups use

---

(1) Sandhu, S. S.; Kohli, K. B.; Brar, A. S. *Inorg. Chem.* **1984**, *23*, 3609.
(2) Ambroz, H. B.; Butter, K. R.; Kemp, T. J. *Faraday Discuss. Chem. Soc.* **1984**, *78*, 107.
(3) Ambroz, H. B.; Kemp, T. J. *J. Chem. Res., Synop.* **1985**, 290.
(4) Shand, M. A. Ph.D. Thesis, University of Warwick, in preparation.
(5) Brar, A. S.; Chander, R.; Sandhu, S. S. *Indian J. Chem., Sect. A* **1979**, *17A*, 554.

0020-1669/86/1325-3840$01.50/0 © 1986 American Chemical Society